NPS ARCHIVE
1968
LOVELAND, K.

VIRTUAL MASS IN STRATIFIED FLUIDS

KENNETH WILDER LOVELAND

DUDLEY KNOX LIBRARY
NAVAL POSTGRADUATE SCHOOL
MONTEREY CA 93943-5101

VIRTUAL MASS

IN

STRATIFIED FLUIDS

by

Kenneth Wilder Loveland
Lieutenant, United States Navy
B.S., United States Naval Academy, 1960

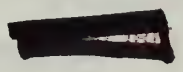

Submitted in partial fulfillment of the
requirements for the degree of

MASTER OF SCIENCE IN MECHANICAL ENGINEERING

from the

NAVAL POSTGRADUATE SCHOOL
June 1968

NRC ARCHIVE
1968
LOVELAND, IC

THESIS
L834 c.1

ABSTRACT

The virtual mass of circular cylinders immersed in a uniformly stratified nonhomogeneous fluid medium has been investigated both theoretically and experimentally. The experimental equipment consisted of a reservoir filled with one inch thick layers of salt water solution. The density uniformly decreased with elevation (stable stratification). The fluid motion about the cylinder was provided by the standing waves created with a plunger. The resulting velocities and accelerations about the cylinder were harmonic. The theoretical analysis consisted of the calculation of the inertia coefficient through the evaluation of the total kinetic energy of the fluid medium. Use was made of the psuedo-potential flow solution for the stratified flow about a circular cylinder. The results have shown that the inertia coefficient for circular cylinders immersed in a uniformly stratified media is about 25% larger than that for a cylinder immersed in an homogeneous medium.

DUDLEY KNOX LIBRARY
NAVAL POSTGRADUATE SCHOOL
MONTEREY CA 93943-5101

TABLE OF CONTENTS

Section		Page
I.	Introduction	13
II.	Previous theoretical and experimental studies	16
III.	Experimental equipment and procedures	20
	Apparatus	20
	Procedures	25
IV.	Theoretical considerations	30
	Virtual Mass in homogeneous fluids	30
	Virtual Mass in nonhomogeneous fluids	31
	Wave characteristics	36
V.	Results	39
VI.	Discussion of results and conclusions	50
VII.	Recommendations	52
VIII.	Bibliography	53

LIST OF TABLES

Table		Page
I.	Fresh water inertia coefficient for one inch cylinder	40
II.	Fresh water inertia coefficient for one and one-half inch cylinder	42
III.	Fresh water inertia coefficient for two inch cylinder	42
IV.	Inertia coefficient for one inch cylinder in stratification No. 1.	43
V.	Inertia coefficient for one and one-half inch cylinder in stratification No. 1.	44
VI.	Inertia coefficient for two inch cylinder in stratification No. 1.	45
VII.	Inertia coefficient for one inch cylinder in stratification No. 2.	46
VIII.	Inertia coefficient for one and one-half inch cylinder in stratification No. 2.	47
IX.	Inertia coefficient for two inch cylinder in stratification No. 2.	48
X.	A comparison of theoretical and experimental inertia coefficients.	49

LIST OF ILLUSTRATIONS

Figure		Page
1.	Overall view of apparatus	19
2.	A schematic drawing of the test apparatus	21
3.	Calibration system	24
4.	Wave form showing stratification	28
5.	Sample recording of amplitude of wave and force on cylinder	39
6.	Flow of a stratified fluid about a circular cylinder	51

NOMENCLATURE

SYMBOL	DEFINITION
A	Area, ft^2 or in^2
a	Amplitude of wave, inches
C_m	Inertia coefficient
C_o	Stream function coefficient
C_4	Stream function coefficient
F	Force, pounds
g	Acceleration of gravity, $ft./sec^2$
H	Mean height of free surface of water above bottom of tank, inches
H_b	Bernoulli "constant"
k	Wave number, sec^{-1}
k*	Added mass coefficient
L	Length of reservoir, inches
M	Mass of cylinder, slugs
m	Added mass, slugs
N_1	Wave equation coefficient
N_2	Wave equation coefficient
p	Pressure, $lb./in.^2$
r	Radial distance from center of cylinder, inches
r_o	Radius of cylinder, inches
r_1	Normalized radial distance, r/r_o
t	Time, seconds
U	Undisturbed velocity of flow or cylinder, ft/sec

u	Horizontal component of velocity in homogeneous medium, ft/sec
u_1	Horizontal component of velocity to left of cylinder, ft/sec
u_2	Horizontal component of velocity to right of cylinder, ft/sec
u'	Horizontal component of velocity in stratified medium, ft/sec
V	Total velocity, ft/sec
v_r	Radial velocity in polar coordinates, ft/sec
v_θ	Tangential velocity in polar coordinates, ft/sec
w	Vertical component of velocity in homogeneous medium, ft/sec
w'	Vertical component of velocity in stratified medium, ft/sec
x	Horizontal coordinate, inches
z	Vertical coordinate, inches
α	Acceleration, ft/sec^2
η'	Vertical component of vorticity
θ	An angle in degrees
ρ	Density, slugs
ρ_o	Density of fluid at cylinder location, slugs
σ	Frequency of oscillations, sec^{-1}
ψ'	Stream function

ACKNOWLEDGEMENT

The author wishes to express his sincere appreciation to Professor T. Sarpkaya for his patience and guidance during the course of the investigation. A special thanks is also due Messrs. Mothersell, Beck, and McKay of the Mechanical Engineering Department who not only did most of the construction work, but also made numerous major changes and minor modifications to the apparatus before its final completion.

I. Introduction.

The purpose of the present investigation is the determination of the virtual mass coefficient for circular cylinders immersed in a uniformly stratified nonhomogeneous medium. Virtual mass, which is a combination of the mass of the body and the added mass resulting from the acceleration of the fluid particles, is of considerable importance in the determination of the resistance of bodies accelerating from rest or decelerating to a full stop. It is for this reason that numerous studies were conducted to elucidate the concept of virtual mass and to determine the appropriate virtual mass coefficients for various shapes of bodies in homogeneous fluid media.

It is necessary to briefly describe various definitions of the added mass concept prior to a description of the work undertaken herewith. As a body is accelerated from rest in a fluid otherwise at rest, the fluid medium surrounding the body is also accelerated. The significant difference between the acceleration of the body and that of the fluid particles is that while the solid body has constant acceleration, the fluid particles have accelerations varying from that of the solid body to zero at an infinite distance from the body. In order to determine the acceleration of the solid body for a given force F exerted on the body, it is, therefore, necessary to know not only the mass of the body but also the integral contribution of the fluid medium surrounding the body. If a volume integral is taken of the local accelerations times the infinitesimal fluid masses and expressed in terms of a lump sum of fluid mass times the constant acceleration of the body, then that lump sum of the fluid mass may be regarded as the mass attached to the

solid body or as increasing the mass of the solid body by this additional mass of fluid. It is for this reason that the mass contributed to the solid body is called the added mass and the sum of the two masses is called the virtual or apparent mass. In other words, the virtual mass is the quotient of the force required to produce the accelerations throughout the fluid divided by the acceleration of the body. In mathematical terms, Newton's second law may thus be written as

$$F = (M + m)\alpha$$

in which M is the mass of the solid body, m the added mass, and α is the acceleration of the solid body. Obviously, in the case when the body is immersed in a fluid medium of very small density such as air, m is negligibly small and thus the equation of motion may be written in its customary form of $F = M\alpha$. In the case where the body is immersed in a fluid of relatively large density such as water, then m becomes quite significant and its neglect may lead to extremely large errors depending on the actual mass of the body. As an example, it is easy to verify that the acceleration of an air bubble will come out to be infinitly large if the added mass is neglected, whereas its true value is twice the acceleration of gravity as would be found through the incorporation of the added mass into the equation of motion.

In operations in large liquid bodies such as in the oceans, one must take into consideration not only the contribution of the added mass in determining the forces acting on the body, but also the effect of the variations in density of the fluid medium on the added mass itself. The studies carried out on added mass in the past were confined to homogeneous fluid media. The advent of underwater technology and the recent progress made in understanding the motion of stratified fluids made it clear that the engineer must have a better understanding of the virtual

mass of various shapes of bodies in nonhomogeneous fluids. It is apparent that there are an infinitely large number of combinations of shapes of bodies and types of liquid nonhomogeneities to be considered. For a scientific approach to the problem, however, one must consider the experimentally and mathematically amenable cases such as the motion of a right circular cylinder in a uniformly stratified fluid medium. It is for this reason that the project described herein investigates the virtual mass of three sizes of circular cylinders in two different but uniformly stratified salt-water solutions through the use of standing waves. The results show, as anticipated theoretically, that the virtual mass coefficients in stratified fluids are about 25% larger than those in homogeneous fluids.

II. Previous Theoretical and Experimental Studies.

The concept of virtual mass was probably first recognized by DuBuat in 1786 while studying the sources of errors in the motion of pendulums. Bessel, in 1826, also recognized the effect in his studies of the same problem. Analytical solutions to the problem were found by Poisson and Green in 1832 and 1836. Froude, in his studies of ship oscillations in 1861, also noticed the added mass effect and took it into account in his inertia coefficient.

Since 1920, there have been a number of papers and texts published concerning added mass, virtual mass, or inertia coefficients. Lamb (1)[1] developed some of the concepts and mathematical background of the virtual mass effect. Landweber and Yih (7) compared the solutions of Lagally, Taylor, and Kirchoff showing their correlation and simplying their proofs. Texts by Rouse (3) and Robertson (2) give clear definitions and theoretical developments of the phenomenon.

Much experimental work on virtual mass has been done in the past 15 years. Keulegan and Carpenter (5) determined inertia coefficients for circular cylinders and flat plates through the use of standing waves. McNown (9) carried out similar studies for lenticular cylinders and flat plates. Sarpkaya (13) conducted studies on the added mass of lenses and parallel plates. Brater et. al. (8) dealt with the determination of the virtual mass coefficients of barges of different geometries. All of these studies have tended to support the theoretically determined virtual mass coefficients for low velocity and small amplitude motions.

[1]Numbers in parenthesis refer to bibliography Section VIII.

As the velocity and amplitudes were increased, departures from the theoretical values were observed. The theoretical analyses invaribly assumed irrotational flow in an ideal, homogeneous, incompressible fluid. Thus it was to be expected that experimental values would differ from those obtained theoretically as separation, vortex formation, and turbulence accompanied the flow following the initial periods of motion. Sarpkaya (13,14) carried out extensive theoretical and experimental studies of the virtual mass and time-dependent resistance for flows with vortex separation.

The previous experimental studies carried out with homogeneous incompressible fluids with bodies either undergoing oscillations of small amplitude or accelerating from rest have shown that the theories of Lagally, Taylor, and Kirchoff are substantially correct provided that the fluid motion does not continue long enough in one direction to cause separation.

The work on the corresponding problem in non-homogeneous fluids, however, has not been as prevalent. Yih (4,12) and Long (10,11) appear to have done most of the work in this field in the past ten years. The most important discovery with regard to virtual mass effect is the phenomenon of "blocking" discussed by Yih (4).

The experiments of Long (11) and Yih (12) indicated that for small amplitude motion stagnation zones occur upstream and sometimes even downstream from a barrier or a moving body. This phenomenon of stratified flow would seem to manifest itself in the form of a "frozen" volume of fluid following the motion of a solid body. Theoretically, there appears to occur a critical regime in which blocking takes place. If the stratification is slight, or the motion rapid, the effect is not noticed. In the present study, the blocking effect per.se. was

not studied, however the relationship between this effect and the virtual mass effect was necessarily taken into account.

From the foregoing, it should be apparent that the blocking would increase the virtual mass coefficient. The validity of this argument has been shown through the experiments presented herein.

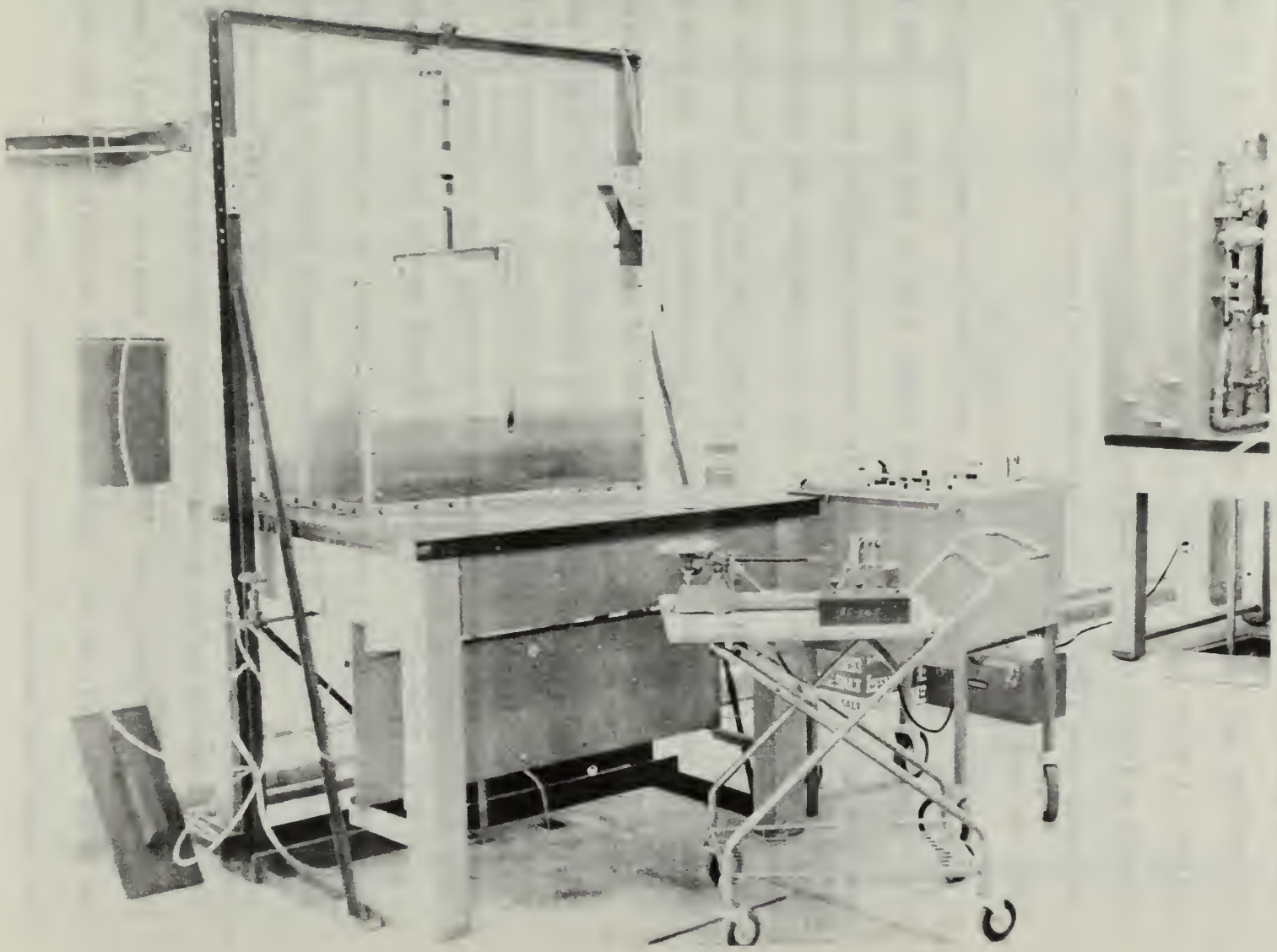

Figure 1 General view of apparatus

III. Experimental Equipment and Procedures.

Equipment

For the experimental study, a one inch thick plexiglas tank with outside dimensions 24" by 24" by 36" was constructed. A ¼ inch hole was drilled and tapped for pipe threads in the center rear of the tank bottom. A three inch diameter circular aluminum flat plate was installed with a 3/16" clearance over this hole. The purpose of the hole was to permit slow filling of the salt-water in layers of varying density from the tank bottom.

A pressure tap was drilled in the side of the tank 4 inches from the top and centered 12 inches from either side of the tank. This tap was made for use with a differential pressure transducer in recording of wave heights. A mounting bracket for the transducer was installed on the outside of the tank in a position such that the zero level of the transducer was located at the level of the pressure tap. One side of the transducer was connected to the tank tap and to a length of tygon tubing in the shape of a standpipe. The standpipe was used as a calibration device. The other side of the differential transducer was left open to atmosphere for the purpose of recording gage pressures.

A heavy steel box frame was constructed around the tank and its supporting table. The base of the frame rested on the concrete floor of the building. The top of the frame was securely bolted to a concrete pillar. The frame was designed so that the height of the cylinder arm could be adjusted in two inch increments. This was accomplished by means of an aluminum bracket which bolted to both sides of the steel frame. The frame was drilled and tapped at two inch intervals from the level of the top of the tank to the top of the frame. (See Fig. 2),

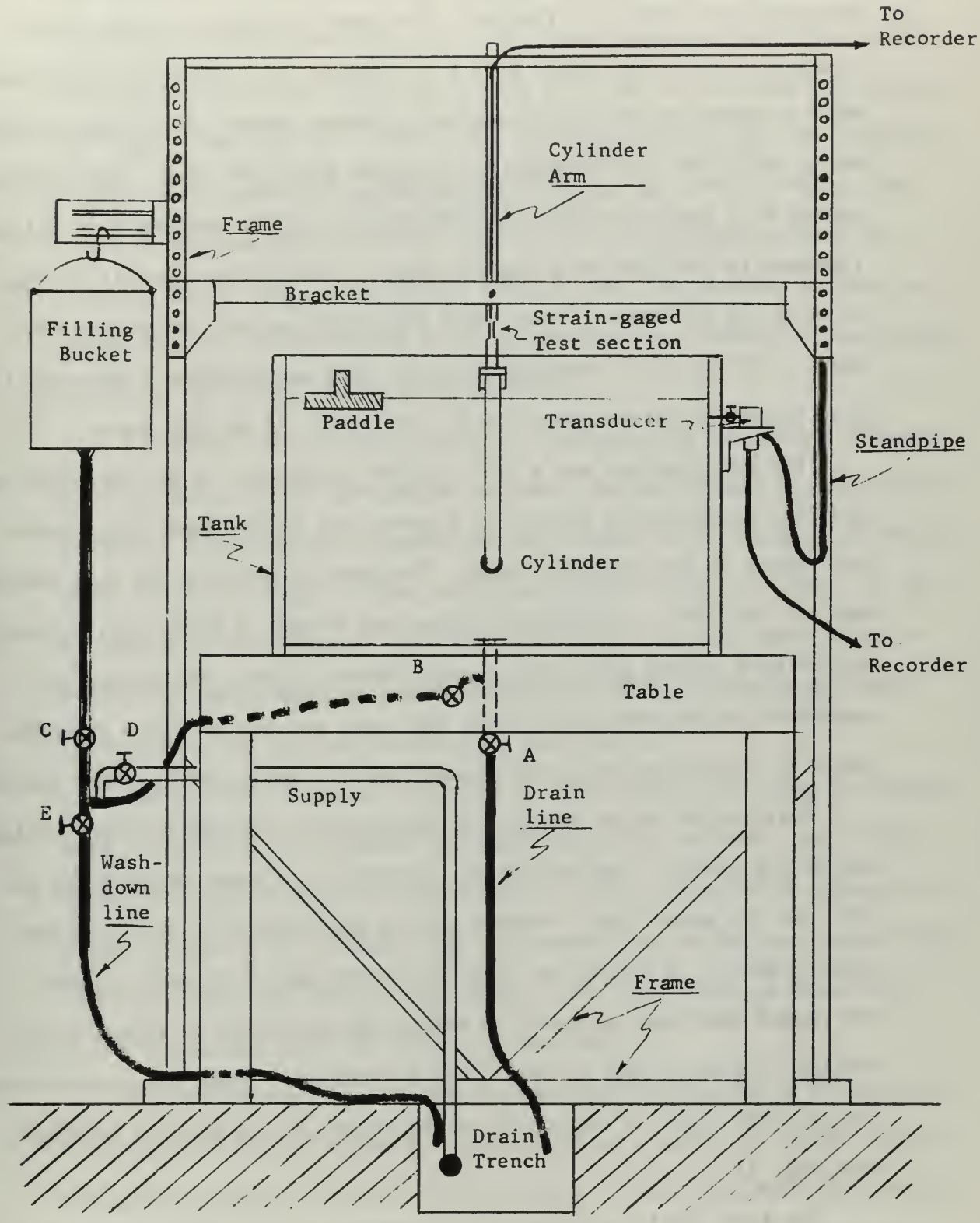

Figure 2. A schematic drawing of the test apparatus

The cylinder arm was attached to the bracket by a gimbal bearing with only one degree of freedom. The upper extension of the arm was clamped to the steel frame with a "C" clamp. The cylinders themselves were attached to the arm by another aluminum frame. This frame consisted of two 1" by 1/8" streamlined aluminum arms, 20" long. The arms were bolted to a top piece which consisted of 1" by ¼" aluminum bars bolted together in the form of a channel beam. The top piece was 21.5" long as were the cylinders. Thus, when the cylinders were bolted to the arms, a 20" by 21.5" rectangular rigid form was produced. This was in turn bolted to the cylinder arm at the center of the top piece.

The cylinder arm was a 3/4" by 7/8" steel rod. A one inch test section was notched into the arm at a point six inches above the attachment point of the cylinder frame. The cross section of the test section was 3/8" by 7/8". A four gage bridge was formed at this section using Microsensor strain gages with a gage factor of 150. The bridge was completed at the test section and the leads brought out in a shielded cable to one channel of a two channel Sanborn amplifier/recorder system.

Calibration of the bridge was accomplished through a pulley, weight, and string system. One pulley was attached to a heavy brass block and set into the empty tank. Another pulley was clamped to the aluminum cross-bracket. A string was attached to the middle of the cylinder and passed over both pulleys. A weight pan was built to attach calibration weights to the string. Thus a horizontal force was produced on the cylinder equal in magnitude to the weight of the pan and weights. (See Fig. 3).

The tank itself was mounted on a heavy 4' by 4' table with a hole in the center rear of the table. A six inch long and ½-inch diameter pipe

was attached to the hole in the bottom of the tank, and supported by a pipe bracket bolted to the table. This pipe extended below the table and was fitted with a valve and tubing fittings for filling or draining the tank. (See Fig. 2). This valve is shown as valve A. The filling tubing ran to valve B located at the front of the table. Tubing from B led to a tee connection at D which was the supply spigot from the building water main. From spigot D tubing was led through another tee either to the filling bucket or to a washdown line. Valves C and E were isolation valves for their respective lines.

A simple filling and mixing bucket was made by punching a hole in the bottom of an old five gallon kerosene can which had been thoroughly cleaned. A fitting was attached to the bottom of the bucket and tubing run from there to the filling system as shown on Fig. 2. Thus, as can be seen from the diagram, by properly manipulating the valve arrangements, the tank could be filled either from the building supply with fresh water, or from the bucket with salt-water.

Salt-water solutions were made in the bucket by filling the bucket with fresh water to a height corresponding to a one inch layer in the tank, then adding measured quantities of salt. In order to increase the pressure head while filling from the bucket, the bucket was raised about six feet above the level of the table. The salt solution could then drain by gravity into the bottom of the tank.

A standing wave was created in the tank by means of a 20 inch by 8 inch piece of ½ inch plywood. Using this as a paddle of sorts, a wave was gently started by hand. The amplitude of the wave was increased by applying a slight lift or push to the paddle in phase with the natural motion of the standing wave in the tank. The plywood was left floating

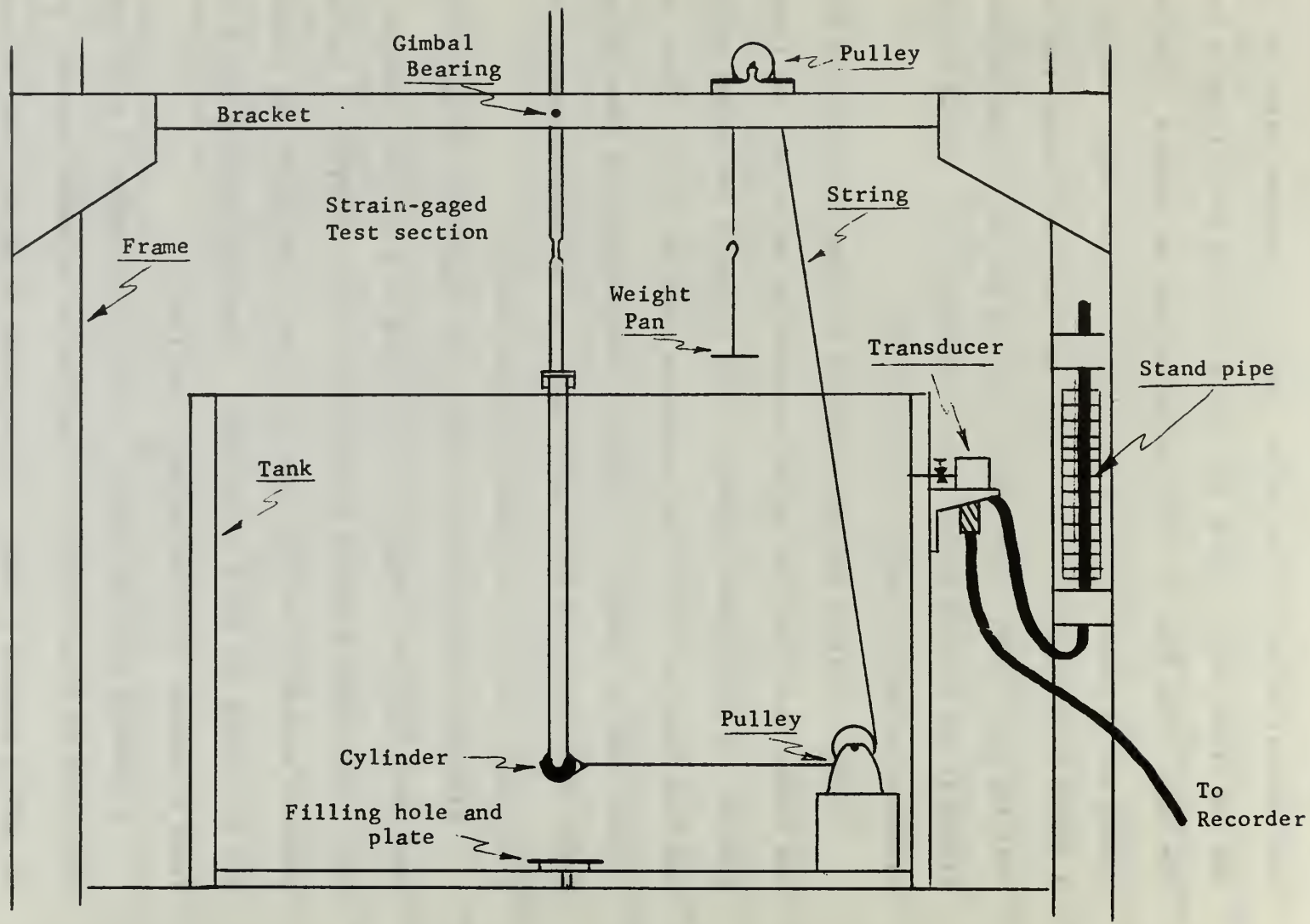

Figure 3 Calibration System

in the tank to help damp out any secondary waves, and because lifting the paddle out of the tank tended to create secondary waves disturbing the basic standing wave pattern.

All readings were taken on a two channel Sanborn amplifier/recorder. This instrument consisted of a Hewlett/Packard model 7712-B recorder with Sanborn model 350-1100C preamplifiers.

Procedures

Prior to conducting the experiments a careful calibration procedure was followed. The first item requiring calibration while the tank was empty was the strain gage bridge and recorder system. This calibration was accomplished by the pulley system previously described and shown in figure 3. With no weights or weight pan on the string, and all tension in the string relaxed, a careful zero balance was obtained on the recorder. Then an accurate weight of 0.1 pounds, including the weight of the pan, was suspended from the string. The needle deflection on the recorder was adjusted by means of the preamplifier gain control so that at an attenuation setting of 10, a deflection of 25 millimeters (half of full scale) was indicated. The weight was then removed and the system zero-balanced again. The above procedure was followed again and checked to insure that the deflection for the same weight and attenuation setting remained constant. All higher attenuation settings were then checked to insure linearity. When this had been accomplished for 0.1 pounds, the weight was changed to 0.2 pounds and the procedure followed again. Once the gain was set during the initial calibration, it was locked in place. Calibration checks were made on both sides of the cylinder, that is the pulley system was shifted to the other end of the tank and calibration repeated for force in that direction. Calibration remained the same for either side of the cylinder.

The tank was then filled to a depth of 19 inches with fresh water. This allowed for one inch of water above the pressure tap in the side of the tank. The transducer pressure side was filled with water from the tank and all air pockets removed from the tubing and transducer cavity. The transducer output was connected to the other channel of the recorder. The recorder was again zero balanced with both the tank valve and the standpipe valve open. The tank stop was then shut and a water column of one inch above tank level was impressed on the transducer by means of the tygon tubing standpipe. The amplifier gain was adjusted for half of full scale deflection with the attenuation setting at 2. The gain on that channel was locked and checks of linearity were made similar to those conducted for the strain-gage arm. Water heights of up to one inch above and below the level of the tank were tested, and the calibration was found to be linear.

Following the completion of the calibrations, a complete system check of the experimental apparatus was made. With fresh water in the tank, runs were made with the 1.0, 1.5, and 2.0 inch diameter cylinders to see how closely the experimentally determined homogeneous fluid virtual mass coefficients agreed with those predicted theoretically. To do this, a standing wave was generated as previously described. Once the fundamental standing wave with no harmonics had been set up, the force acting on the cylinder and the wave heights at the end of the tank were simultaneously recorded.

Immediately after each experiment, the transducer calibration was checked. It was found that the gain setting needed no changes throughout the series of experiments. The water was then drained out of the tank and the strain-gage arm calibration checked again as above. Again,

no change was required from the initial calibration setting in spite of changing of the cylinders.

When all the runs had been completed with fresh water, the water was drained out of the reservoir, calibrations were repeated, and the stratified layers were introduced into the tank. This was accomplished by slowly filling the water-salt solution from the bottom of the tank through the filling system previously described. The first layer to be introduced was two inch layer of fresh water. The solutions for the second and succeeding layers were prepared by filling the bucket and adding a measured quantity of salt (10 milliliters or 30 milliliters) and mixing thoroughly. The quantity of salt was increased by equal amounts for each succeeding layer, that is, 10 ml. for the second layer, 20 ml. for the third, 30 ml. for the fourth, etc. As each solution was mixed in the bucket it was dyed with red, blue, or black ink, or on occasions was left clear for contrast. The purpose of the dye was merely to make the layers visible. Once the salt, water, and dye had been mixed and the salt completely dissolved, the specific gravity of the solution was determined with a hydrometer. The bucket was then raised to an elevation 6 feet above the level of the reservoir, and the valves opened to allow draining of the bucket into the bottom of the tank.

The flat plate over the filling hole allowed the slow radial diffusion of the entering solution, preventing premature or undesirable mixing of the successive layers. As the new, more dense layer entered the bottom of the tank and spread radially from the filling hole, it lifted the less dense layers above it. This process was continued until the tank had been filled to a water depth of approximately 19 inches. Once the filling process was completed, the tank was allowed to sit for a day

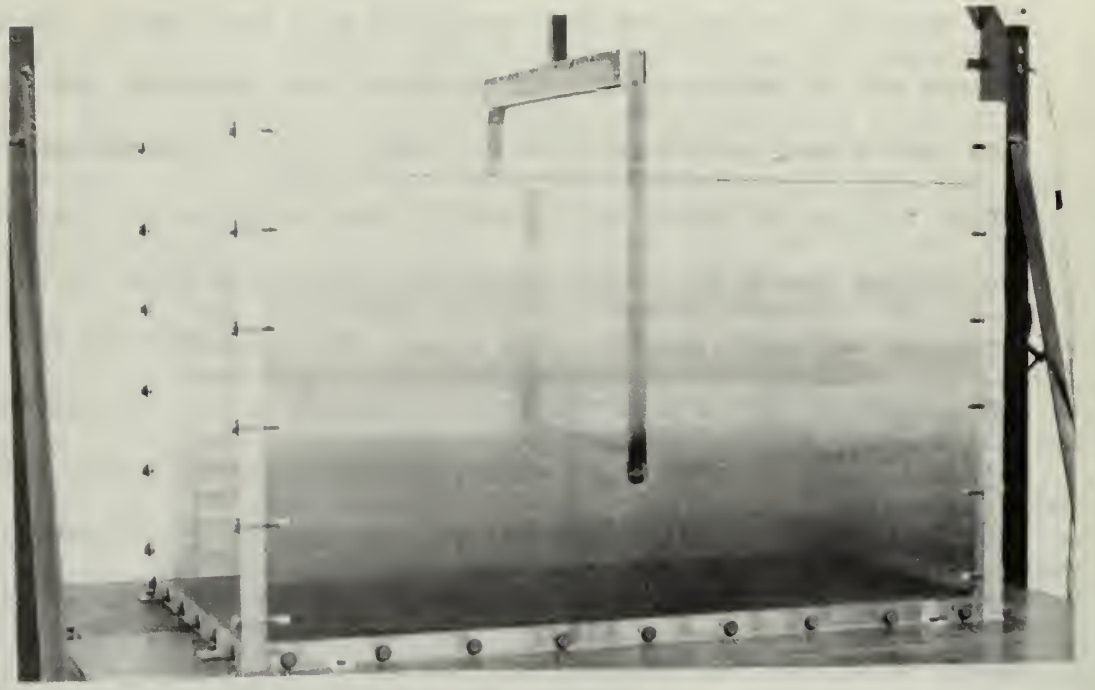

Figure 4(a) Stratified Layers

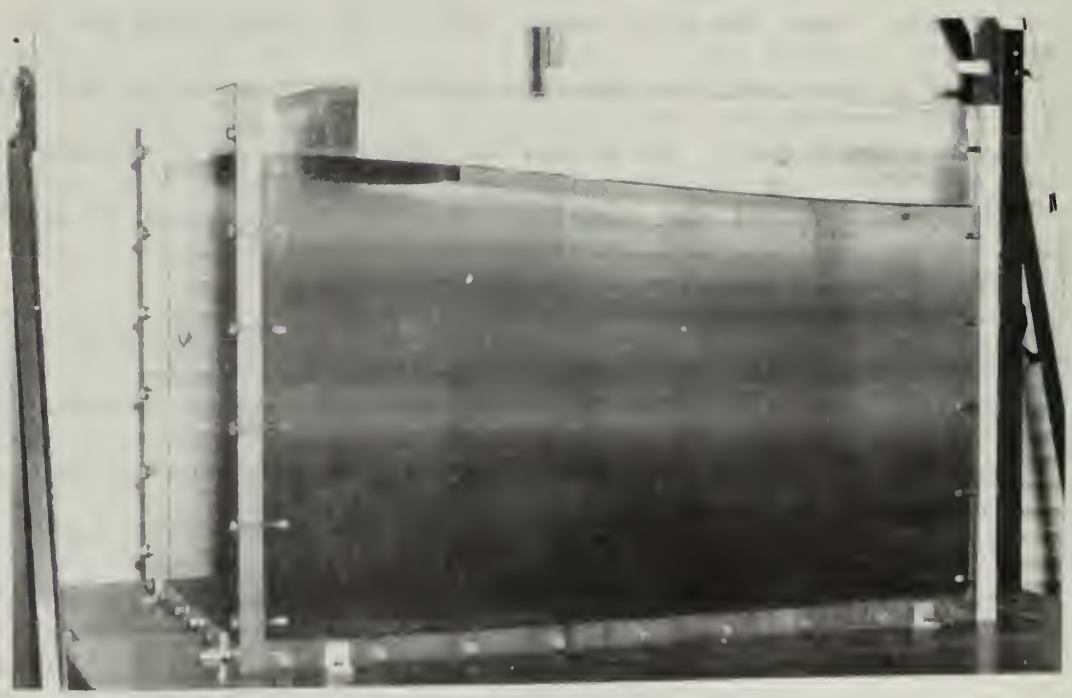

Figure 4(b) Wave Form

or so prior to the start of the tests. This waiting period allowed molecular diffusion to take place producing a uniform density gradient rather than a step layer effect. Each one inch layer took approximately 20 minutes to prepare, and an hour to drain into the tank. The entire filling procedure took a period of three days.

Once the tank was filled with the stratified salt-water, the calibration of the transducer was checked as previously described. A standing wave was set up in the tank. The forces acting on the cylinder and the wave amplitudes were recorded. Two density gradients and three different cylinder diameters were used in the experiments. From these data the virtual mass coefficients of cylinders in both the homogeneous and stratified fluid media were calculated.

IV. Theoretical Considerations.

1. Added Mass and Inertia Coefficients (Homogeneous Fluid)

The force exerted on a circular cylinder by an inviscid fluid of velocity U and acceleration dU/dt may be determined as follows:

Letting U be the undisturbed velocity of the ambient flow, the velocity components for the flow about the cylinder are given by (See Lamb)

$$u = U\left(1 + \frac{r_o^2}{r^2}\cos 2\theta\right)$$

$$w = -U\frac{r_o^2}{r^2}\sin 2\theta \qquad (1)$$

The pressure at any point in the fluid medium reduces to:

$$\frac{p}{\rho} = \frac{dU}{dt}\left(r + \frac{r_o^2}{r}\right)\sin\theta - \frac{1}{2}(u^2 + w^2) \qquad (2)$$

Writing the equation of momentum in its familiar form

$$F = -\rho\int_A \frac{\partial u}{\partial t}\,dA + \rho\int_{-\infty}^{\infty}(u_1^2 - u_2^2)dx + \int_{-\infty}^{\infty}(p_1 - p_2)dx \qquad (3)$$

and noting that for the case under consideration, $u_1 = u_2$ at infinity, i.e., the flow is symmetrical, we have

$$F = -\rho\int_A \frac{\partial u}{\partial t}\,dA + \int_{-\infty}^{\infty}(p_1 - p_2)\,dx \qquad (4)$$

It is apparent that the force acting on the cylinder in the absence of a pressure gradient is given by the first term on the right hand side of equation (4). This corresponds to the case where the fluid is at rest and the cylinder is moving with the time dependent velocity U. Because of this obvious difference between the acceleration of flow about a cylinder at rest and the acceleration of the cylinder in a fluid at rest, two types of force coefficients are employed in the literature.

The normalized force coefficient for the case corresponding to the acceleration of the fluid is called the inertia coefficient, and the one corresponding to the acceleration of the cylinder, the added mass coefficient. As will be seen later, the two coefficients differ only and always by a constant equal to 1.0.

Inserting equations (1) and (2) into equation (4) and performing the indicated integrations, we have

$$F = \pi \rho r_o^2 \frac{dU}{dt} + \pi \rho r_o^2 \frac{dU}{dt} \tag{5}$$

Normalizing equation (5) by "displaced mass times acceleration", yields

$$\frac{F}{\pi \rho r_o^2 \frac{dU}{dt}} = C_m = 2 \tag{6}$$

where C_m is known as the inertia coefficient. It is obvious that in the case of a circular cylinder accelerating in a fluid otherwise at rest k* = 1, k* being the added mass coefficient. For other shapes of bodies, k* differs from unity and C_m reduces to: $C_m = k^* + 1$. In passing it should be noted that for a sphere $C_m = 1.50$, provided that the flow about the sphere is unseparated.

In the present investigation, the cylinder is at rest and the theoretical value of the inertia coefficient for an homogeneous working fluid is $C_m = 2.0$. This will later be compared with those obtained experimentally and it will be shown that there is excellent agreement between the theoretical prediction and the measured values.

2. Added Mass Coefficients (Nonhomogeneous Fluid).

The equations of motion for a nonhomogeneous fluid will first

be summarized prior to the evaluation of the added mass coefficient for a circular cylinder immersed in a uniformly stratified fluid medium.

The equation of continuity may be written as

$$\frac{\partial u'}{\partial x} + \frac{\partial w'}{\partial z} = 0 \tag{7}$$

where

$$u' = \sqrt{\frac{\rho}{\rho_0}}\, u \quad \text{and} \quad w' = \sqrt{\frac{\rho}{\rho_0}}\, w \tag{8}$$

The stream function ψ' is given by

$$u' = \frac{\partial \psi'}{\partial z} \quad \text{and} \quad w' = -\frac{\partial \psi'}{\partial x} \tag{9}$$

The equations of motion, in terms of u' and w', become

$$\rho_0\left(u'\frac{\partial u'}{\partial x} + w'\frac{\partial u'}{\partial z}\right) = -\frac{\partial p}{\partial x} \tag{10}$$

and

$$\rho_0\left(u'\frac{\partial w'}{\partial x} + w'\frac{\partial w'}{\partial z}\right) = -\frac{\partial p}{\partial z} - g\rho \tag{11}$$

Writing the Bernoulli constant H_b as

$$H_b = p + \frac{\rho(u^2+w^2)}{2} + \rho g z \tag{12}$$

and the z - component of vorticity η' as

$$\eta' = \frac{\partial u'}{\partial z} - \frac{\partial w'}{\partial x} = \nabla^2 \psi' \tag{13}$$

equations (10) and (11) may be written as

$$\nabla^2 \psi' + \frac{g z}{\rho_0} \cdot \frac{\partial \rho}{\partial \psi'} = \frac{dH_b}{d\psi'} \tag{14}$$

The foregoing equation was derived by Long (11) and Yih (4).

Equation (14) may be used in the study of a class of psuedo-potential flows. One such flow case is the motion of a circular cylinder in a uniformly stratified fluid. The stream function for the case under consideration has been given by Yih (4) as follows:

$$\psi' = \frac{C_0}{24} r_0^3 \left(\frac{3 \sin\theta}{r_1} - \frac{\sin 3\theta}{r_1^3} \right) - C_4 \frac{r_0}{r_1} \sin\theta \tag{15}$$

in which $r_1 = r/r_0$, r_0 being the radius of the cylinder, $C_4 = U$, the velocity of the cylinder, and

$$C_0 = 2\sqrt{6} \frac{U}{r_0} \left(1 - \frac{r_0}{\rho_0} \frac{d\rho}{dz} \right) \tag{16}$$

The added mass coefficient may be calculated through the use of equation (15) by evaluating the velocity components and performing the integration for the kinetic energy as

$$T = 2 \int_{r_0}^{\infty} \int_{0}^{\pi} \frac{1}{2} \rho V^2 r \, dr \, d\theta \tag{17}$$

and noting that in

$$T = \frac{1}{2} m U^2 \tag{18}$$

m is the added mass sought.

The velocity components in polar coordinates are obtained from

equation (15) as

$$V_r = \frac{1}{r}\frac{\partial \psi'}{\partial \theta} = \frac{C_0 r_0^3}{8}\left(\frac{r_0}{r^2}\cos\theta - \frac{r_0^3}{r^4}\cos 3\theta\right) - C_4 \frac{r_0^2}{r^2}\cos\theta \tag{19}$$

$$V_\theta = -\frac{\partial \psi'}{\partial r} = \frac{C_0 r_0^3}{8}\left(\frac{r_0}{r^2}\sin\theta - \frac{r_0^3}{r^4}\sin 3\theta\right) + C_4 \frac{r_0^2}{r^2}\sin\theta \tag{20}$$

Evaluating the total velocity, we have

$$\begin{aligned} V^2 = V_r^2 + V_\theta^2 = \frac{C_0 r_0^3}{8}\Bigg\{ & \frac{r_0^2}{r^4} + \frac{r_0^6}{r^8} - 2\frac{r_0^4}{r^6}\cos\theta\cos 3\theta \\ & - 2\frac{r_0^4}{r^6}\sin\theta\sin 3\theta\Bigg\} - \frac{C_0 C_4 r_0^5}{8r^2}\left(\frac{r_0}{r^2}\cos^2\theta\right. \\ & \left. - \frac{r_0^3}{r^4}\cos\theta\cos 3\theta\right) + \frac{C_0 C_4 r_0^5}{8r^2}\left(\frac{r_0}{r^2}\sin^2\theta\right. \\ & \left. - \frac{r_0^3}{r^4}\sin\theta\sin 3\theta\right) + C_4^2\frac{r_0^4}{r^4} \end{aligned} \tag{21}$$

Obviously, the integration of the terms involving sin θ sin 3θ, cos θ cos 3θ through the use of equation (17) between the limits indicated shows that these terms have no contribution. Furthermore, the integration of the terms involving $\cos^2\theta$ and $\sin^2\theta$ cancel each other out due to the opposite signs of their coefficients. The remaining terms, i.e., the first, second, and the last term on the right hand side of equation (21) yield

$$T = \frac{1}{2}\pi\rho_0 r_0^2 C_4^2 + \frac{1}{2}\left(\pi\rho_0 \frac{C_0^2}{48}\frac{r_0^6}{U^2}\right)U^2 \qquad (22)$$

Hence the added mass m reduces to

$$m = \pi\rho_0 r_0^2 + \frac{\pi\rho_0}{48} C_0^2 \frac{r_0^6}{U^2} \qquad (23)$$

Inserting the value of C_0 from equation (16) into equation (23) and dividing by the displaced mass of the cylinder i.e., $\pi\rho_0 r_0^2$,we have the added mass coefficient k*, as

$$k^* = 1 + \frac{1}{2}\left(1 - \frac{r_0}{\rho_0}\frac{d\rho}{dz}\right)^2 \qquad (24)$$

It should be noted that for a density stratification where ρ is decreasing with elevation (stable stratification), $d\rho/dz$ is negative.

The inertia coefficient C_m , which was given by $C_m = k^* + 1$, now reduces to

$$C_m = 2 + \frac{1}{2}\left(1 - \frac{r_0}{\rho_0}\frac{d\rho}{dz}\right)^2 \qquad (25)$$

The results obtained from equation (25) will be compared in the next section with those obtained experimentally. It suffices to note that in stratified flows the inertia coefficients depend, unlike homogeneous fluids, on the density of fluid, the radius of the cylinder, and of course on the density gradient.

3. Characteristics of the Experimental Waves.

The region under the nodal area of a standing wave that may be realized in a rectangular tank provides a velocity field of simple harmonic motion in the velocity component U.

Taking the x-axis in the plane surface of the undisturbed water, the z axis vertical and upwards, and the origin at one end of the tank, the surface elevation, measured from the undisturbed level, is given by Miche (6) to a second order of approximation in the amplitude as:

$$h = a \cos kx \sin \sigma t + \frac{a^2 k}{4} N_1 \cos 2kx - \frac{a^2 k}{4} N_2 \cos 2kx \cos 2\sigma t \qquad (26)$$

where $$N_1 = \frac{\cosh 2kH}{\sinh 2kH}$$

and $$N_2 = \frac{\cosh^2 kH \,(\cosh 2kH + 2)}{\sinh^2 kH \sinh kH}$$

where $k = \pi/L$, L being the length of the basin; $\sigma = 2\pi/T$, T being the period of oscillation; H the depth of water; and a the semi-wave height, that is the mean value of the extreme end deflections in a cycle.

The period is related to k and H by the expression

$$\sigma^2 = gk \tanh kH \qquad (27)$$

The surface elevation at x = 0, at any time, becomes

$$h = a \sin \sigma t + \frac{a^2 k}{4} N_1 - \frac{a^2 k}{4} N_2 \cos 2\sigma t \qquad (28)$$

The expressions for the particle velocities, within the order of the approximations considered, are given by Miche (6) as

$$u = -\frac{gak}{\sigma}\,\frac{\cosh k(z+H)}{\cosh kH}\,\sin kx\,\cos\sigma t - \frac{3}{4}\,\frac{ga^2k^2}{\sigma}\,\frac{\cosh 2k(z+H)}{\sinh^2 kH \sinh 2kH}\,\sin 2kx\,\sin 2\sigma t \tag{29}$$

and

$$w = \frac{gak}{\sigma}\,\frac{\sinh k(z+H)}{\cosh kH}\,\cos kx\,\cos\sigma t + \frac{3}{4}\,\frac{ga^2k^2}{\sigma}\,\frac{\sinh 2k(z+H)}{\sinh^2 kH \sinh 2kH}\,\cos kx\,\sin 2\sigma t \tag{30}$$

At the vertical plane through the midsection of the tank, i.e., at the plane x = L/2 or kx = $\pi/2$, the velocities become

$$u = -\frac{gak}{\sigma}\,\frac{\cosh k(z+H)}{\cosh kH}\,\cos\sigma t \tag{31}$$

and

$$w = -\frac{3}{4}\,\frac{ga^2k^2}{\sigma}\,\frac{\sinh 2k(z+H)}{\sinh^2 kH \sinh kH}\,\sin 2\sigma t \tag{32}$$

Obviously, the horizontal component of velocity at the channel midsection is simple harmonic. The vertical component is also simple harmonic except that the frequency is twice as large. The effect of the vertical velocity is negligibly small and decreases with both the wave height and the lowering of the cylinder in the reservoir. The majority of the experiments were made with "a" less than 0.5 inch. For these cases the ratio of the amplitudes of vertical and horizontal components of velocity, w_m/u_m, at the cylinder location was found to be 0.004.

The acceleration at the nodal plane may be obtained from equation (31)

$$\frac{dU}{dt} = gak \frac{\cosh k(z+H)}{\cosh kH} \sin \sigma t \qquad (33)$$

Clearly, acceleration reaches its maximum value when the velocity reaches its minimum value of zero and vice-versa. This observation constitutes one of the most significant points of the experimental procedure. It is a well known fact that the prediction of the forces attributable to drag and to virtual mass is quite complex for flows in which separation takes place. At moments of maximum acceleration and zero velocity, there is no wake, and the pattern of flow closely resembles that for irrotational flow without separation. The foregoing discussion and analysis explain the reason for the selection of a simple-harmonic wave motion in the determination of virtual mass of a circular cylinder or, for that matter, of any other object.

V. Results.

The following tables present representative values obtained during the course of the experiments. The following procedure was used in the determination of the inertia coefficient:

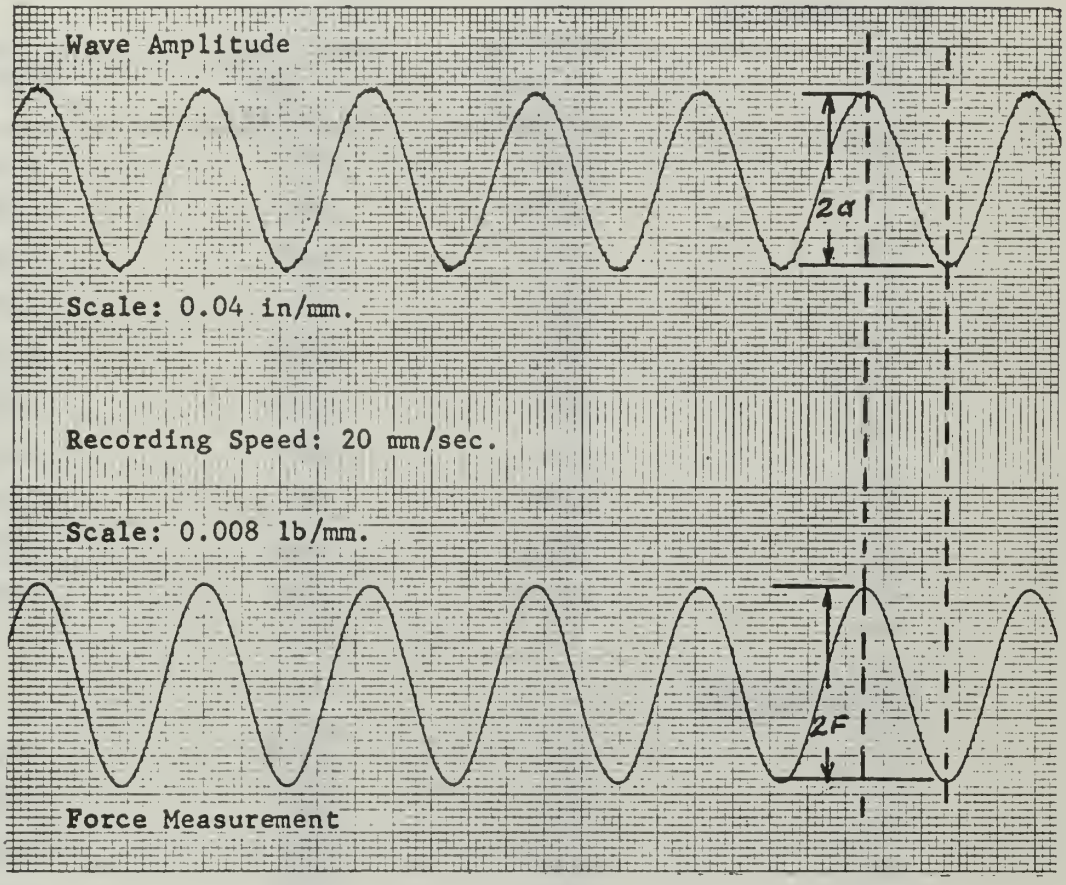

Figure 5. Sample recording of amplitude of wave and force on cylinder.

1. Inserting the measured amplitude of the wave and the appropriate values of k, H, and z into equation (33), noting that the amplitude was taken at its maximum when cos (σ t) = 1, the amplitude of the acceleration was calculated;

2. Using the corresponding measured values of the amplitude of force, the inertia coefficient was calculated from equation (6).

TABLE I

Results of system check with fresh water

Cylinder diameter: 1 inch
Water depth: 19 inches
Height of cylinder above bottom: 4.375 inches

RUN NUMBER ONE

Point	Force on cylinder (pounds)	Amplitude of wave (inches)	Inertia Coefficient
1	.0124	.281	2.154
2	.00976	.25	1.906
3	.0092	.2187	2.054
4	.008	.212	1.842
5	.0072	.1875	1.875
6	.006	.141	2.077
7	.006	.141	2.077
8	.0044	.105	2.046
9	.0036	.0937	1.876
10	.00264	.0625	2.062

RUN NUMBER TWO

1	.018	.4225	2.080
2	.016	.406	1.924
3	.0145	.360	1.966
4	.0128	.328	1.905
5	.0116	.282	2.008
6	.0104	.250	2.031
7	.0092	.235	1.911
8	.0083	.208	1.948
9	.00575	.141	1.991
10	.0048	.1158	2.023

TABLE I (continued)

Results of system check with fresh water

RUN NUMBER THREE

Point	Force on cylinder (pounds)	Amplitude of wave (inches)	Inertia Coefficients
1	.032	.750	2.085
2	.029	.720	1.968
3	.027	.666	1.981
4	.0255	.610	2.043
5	.0235	.579	1.983
6	.0212	.506	2.047
7	.0206	.500	2.015
8	.0185	.445	2.032
9	.017	.406	2.046
10	.015	.375	1.955
11	.0136	.344	1.932
12	.0124	.312	1.942
13	.0114	.281	1.982
14	.0098	.250	1.916
15	.0094	.219	2.098
16	.0084	.203	2.022
17	.0078	.1875	2.033
18	.0065	.1562	2.034
19	.0058	.1407	2.015
20	.0052	.125	2.033

TABLE II

Results of system check with fresh water

Cylinder diameter 1.5 inches
Water depth: 19 inches
Height of cylinder above bottom: 6.5 inches

Point	Force on cylinder (pounds)	Amplitude of wave (inches)	Inertia Coefficient
1	.0146	.150	1.957
2	.024	.25	1.930
3	.026	.275	1.901
4	.0375	.388	1.943
5	.040	.413	1.947
6	.0415	.425	1.963
7	.020	.200	2.010
8	.0218	.225	1.948
9	.0300	.3125	1.930
10	.034	.338	2.022

TABLE III

Cylinder diameter: 2 inches
Water depth: 18.875 inches
Height of cylinder above bottom: 8.5 inches

1	.058	.272	2.097
2	.055	.272	1.988
3	.052	.247	2.070
4	.030	.147	2.007
5	.029	.136	2.097
6	.080	.358	2.198
7	.070	.321	2.144
8	.062	.297	2.053
9	.038	.185	2.020
10	.024	.124	1.903

TABLE IV

Results in stratified salt-water

Density gradient: .000020 #/in^4
Water depth: 19.5 inches
Cylinder diameter: 1 inch
Height of cylinder above bottom: 6.5 inches

Point	Force on cylinder (pounds)	Amplitude of wave (inches)	Inertia Coefficient
1	.0309	.51	2.83
2	.0298	.48	2.90
3	.0270	.46	2.74
4	.0258	.425	2.84
5	.024	.40	2.80
6	.0222	.37	2.80
7	.0205	.35	2.74
8	.0195	.32	2.85
9	.0172	.30	2.68
10	.0120	.21	2.67
11	.0116	.20	2.71
12	.010	.175	2.67
13	.009	.16	2.63
14	.008	.13	2.88
15	.0073	.12	2.84
16	.032	.52	2.87
17	.0289	.495	2.72
18	.026	.43	2.82
19	.0245	.395	2.89
20	.0173	.29	2.79
21	.160	.26	2.87
22	.0142	.24	2.76

TABLE V

Results in stratified salt-water

Density gradient: .000020 #/in^4
Water depth: 19.5 inches
Cylinder diameter: 1.5 inches
Height of cylinder above bottom: 6.5 inches

Point	Force on cylinder (pounds)	Amplitude of wave (inches)	Inertia Coefficient
1	.0475	.38	2.64
2	.048	.36	2.78
3	.046	.36	2.68
4	.044	.362	2.53
5	.035	.28	2.60
6	.0322	.25	2.68
7	.029	.24	2.52
8	.0263	.20	2.74
9	.022	.18	2.54
10	.0198	.16	2.58
11	.075	.61	2.56
12	.072	.58	2.58
13	.068	.54	2.62
14	.064	.50	2.66
15	.0585	.46	2.65
16	.055	.44	2.60
17	.052	.415	2.61
18	.049	.40	2.56
19	.046	.365	2.62
20	.0365	.29	2.62
21	.028	.22	2.65
22	.023	.18	2.66

TABLE VI

Results in stratified salt-water

Density gradient: .000020 #/in^4
Water depth: 19.5 inches
Cylinder diameter: 2 inches
Height of cylinder above bottom: 6.5 inches

Point	Force on cylinder (pounds)	Amplitude of wave (inches)	Inertia Coefficient
1	.096	.44	2.56
2	,088	.40	2.35
3	.080	.36	2.60
4	.073	.345	2.48
5	.0645	.29	2.60
6	.0565	.265	2.50
7	.054	.26	2.44
8	.046	.22	2.45
9	.0392	.18	2.55
10	.036	.16	2.64
11	.0335	.16	2.46
12	.0295	.135	2.56
13	.0275	.12	2.68
14	.025	.11	2.66
15	.0225	.10	2.64
16	.146	.66	2.59
17	.107	.47	2.67
18	.078	.35	2.61
19	.0405	.18	2.63
20	.0265	.12	2.58
21	.094	.42	2.62
22	.038	.17	2.62

TABLE VII

Results in stratified salt-water

Density gradient: .000042 #/in^4
Cylinder diameter: 1 inch
Water depth: 19.5 inches
Height of cylinder above bottom: 6.5 inches

Point	Force on cylinder (pounds)	Amplitude of wave (inches)	Inertia Coefficient
1	.0134	.21	2.94
2	.0133	.215	2.85
3	.0104	.18	2.66
4	.010	.16	2.88
5	.0093	.15	2.85
6	.008	.13	2.83
7	.0435	.71	2.82
8	.0405	.67	2.78
9	.0355	.58	2.82
10	.0265	.44	2.77
11	.026	.42	2.85
12	.0245	.40	2.82
13	.0232	.38	2.81
14	.022	.36	2.81
15	.020	.32	2.88
16	.019	.30	2.91
17	.0172	.28	2.83
18	.0154	.25	2.83
19	.014	.23	2.80
20	.0132	.22	2.76

TABLE VIII

Results in stratified salt-water

Density gradient: .000042 #/in^4
Cylinder diameter: 1.5 inches
Water depth: 19.5 inches
Height of cylinder above bottom: 6.5 inches

Point	Force on cylinder (pounds)	Amplitude of wave (inches)	Inertia Coefficient
1	.06	.47	2.60
2	.058	.44	2.69
3	.055	.43	2.61
4	.052	.40	2.65
5	.050	.38	2.69
6	.046	.36	2.61
7	.0435	.34	2.61
8	.0417	.33	2.58
9	.0403	.305	2.69
10	.0375	.295	2.59
11	.0356	.28	2.59
12	.0325	.26	2.56
13	.0295	.24	2.51
14	.026	.21	2.52
15	.025	.20	2.55
16	.0158	.13	2.48
17	.0108	.09	2.45
18	.084	.63	2.72
19	.063	.50	2.57
20	.049	.39	2.56

TABLE IX

Results in stratified salt-water

Density gradient: .000042 #/in^4
Cylinder diameter: 2 inches
Water depth: 19.5 inches
Height of cylinder above bottom: 6.5 inches

Point	Force on cylinder (pounds)	Amplitude of wave (inches)	Inertia Coefficient
1	.141	.64	2.54
2	.130	.58	2.58
3	.110	.50	2.53
4	.103	.45	2.63
5	.092	.41	2.58
6	.078	.36	2.49
7	.069	.315	2.52
8	.060	.27	2.56
9	.052	.245	2.44
10	.042	.20	2.42
11	.0385	.18	2.46
12	.036	.17	2.44
13	.0315	.15	2.42
14	.100	.45	2.56
15	.080	.365	2.52
16	.067	.29	2.66
17	.0565	.26	2.50
18	.0485	.22	2.535
19	.037	.16	2.66
20	.026	.12	2.49

TABLE X

A comparison of theoretical and experimental inertia coefficients.

Experimental values are means of numerous points taken during several runs. Note the very slight effect of the cylinder size and density stratification on the theoretical values of inertia coefficients.

Cylinder size (inches)	Inertia coefficients: Theoretical value	Inertia coefficients: Experimental mean
	Fresh water	
1.0	2.000	1.998
1.5	2.000	1.910
2.0	2.000	2.094
	First stratification, gradient 0.00002 #/in^4	
1.0	2.500275	2.78
1.5	2.500413	2.61
2.0	2.500550	2.565
	Second stratification, gradient 0.000042 #/in^4	
1.0	2.500715	2.834
1.5	2.501074	2.508
2.0	2.501433	2.509

VI. Discussion of Results and Conclusions.

The experimental data tabulated in tables I-X have shown that the inertia coefficient for circular cylinders depends on the density of the fluid and to a lesser extent on the density gradient and the diameter of the cylinder. For reasons yet unknown the inertia coefficients for the one inch cylinder are about 15% higher than those for the 1.5 and 2 inch cylinders. The values calculated with the appropriate values for the density, density gradient, and the diameter of the cylinder through the use of equation (24) gave an inertia coefficient of 2.5 as shown in Table X. This value varied very slightly with either the density gradient or the cylinder size. It is, therefore, apparent from a comparison of the theoretical value with those obtained experimentally that the theoretical value is somewhat lower than those predicted experimentally. Among several reasons which could be provided, one is that the stratified fluid medium is confined and that this confinement, unlike in the case of homogeneous fluids, affects more adversely the blockage effect cited earlier. Additional errors may have come from the deviations of the density gradient from uniformity and from the presence of the connecting arms extending through a stratified media. Nevertheless, the agreement between the theory and experiments is sufficiently good to conclude that the inertia coefficient for a circular cylinder immersed in a stratified fluid media is about 25% larger than that in a homogeneous media. The consequences of the increase of the inertia coefficient are rather apparent when one considers the fact that in such media as the oceans, and in particular in layers close to the thermocline, the acceleration of a body requires a proportionally larger amount of power.

In the foregoing we have discussed so far the theoretical and experimental values of the inertia coefficients as they were calculated or measured, but did not elaborate on the reasons as to why such an increase should occur. A careful analysis of the flow about a circular cylinder immersed in a stratified fluid medium (See Fig. 6) shows that there are six instead of two stagnation points about the cylinder.

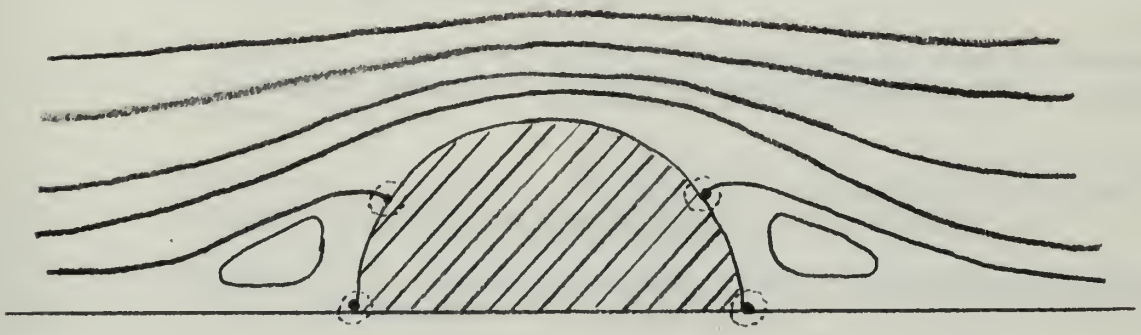

Figure 6. Flow of a stratified fluid about a circular cylinder.

Furthermore, there are on both sides of the cylinder two roughly triangular eddies symmetrically located with respect to either axis. It is apparent that the presence of additional stagnation points and the wedge shaped fluid body in the front and rear of the cylinder would necessarily increase the added mass and hence the inertia coefficient.

In conclusion, it suffices to state that the inertia coefficient for cylinders immersed in a stratified fluid medium depends on the size of the cylinder, the density gradient, and the density of the fluid, and that the inertia coefficient is about 25% larger than that of a cylinder immersed in an homogeneous medium.

VII. Recommendations for further Studies.

It is strongly recommended that the project described herein be extended to flat plates, spheres, and other three dimensional bodies through the use of the same experimental apparatus. Even though an analysis of the stratified flow about a three dimensional body may be rather difficult, it is believed that an analysis similar to that presented here may be carried out for a flat plate vertically placed in the reservoir, i.e., normal to the direction of the horizontal component of the velocity.

BIBLIOGRAPHY

1. Lamb, Sir Horace. Hydrodynamics, Dover Pub., 1932.

2. Robertson, J. H. Hydrodynamics in Theory and Practice. Prentice-Hall, 1965.

3. Rouse, H. Advanced Mechanics of Fluids. Wiley, 1959.

4. Yih, C. S. Dynamics of Nonhomogeneous Fluids. Macmillan, 1965.

5. Keulegan, G. H., and Carpenter, L. H. "Forces on Cylinders and Plates". Nat. Bureau of Stds. Report No. 4821, 1956.

6. Miche, M. "Mouvements Ondulatoires de la mer en profondeur constante ou decroissante," Annales des Ponts et Chaussees, Vol. 114, pp. 25-406, 1944.

7. Landweber, L. and Yih, C. S. "Forces, Moments, and Added Masses for Rankine Bodies". Journal of Fluid Mechanics, Vol. 1, pp. 319-36, 1956.

8. Brater, E. F., et.al. "Wave Forces on Submerged Structures". Journal of the Hydraulics Division, ASCE, 1958.

9. McNown, J. S. "Drag in Unsteady Flow". International Congress of Applied Mechanics, Brussels, 1956.

10. Martin, S. and Long, R. R. "The Slow Motion of a Flat Plate in a Viscous Stratified Fluid". Journal of Fluid Mechanics, Vol. 31, pp. 669-88, 1968.

11. Long, R. R. "The Motions of Fluids with Density Stratifications". Journal of Geophysical Research, Vol. 64, pp. 2151-63, 1959.

12. Yih, C. S. "The Effect of Density Variations on Fluid Flow". Journal of Geophysical Research, Vol. 64, pp. 2219-23, 1959.

13. Sarpkaya, T. "Added Masses of Lenses and Parallel Plates". Journal of the Engineering Mechanics Division, ASCE, Vol. 86, pp. 137-50, 1960.

14. Sarpkaya, T. "An Analytical Study of Separated Flow About Circular Cylinders". ASME Paper No. 68-FE-15, 1968.

INITIAL DISTRIBUTION LIST

		No. Copies
1.	Defense Documentation Center Cameron Station Alexandria, Virginia 22314	20
2.	Library Naval Postgraduate School Monterey, Calif.	2
3.	Professor T. Sarpkaya Chairman, Department of Mechanical Engineering Naval Postgraduate School Monterey, Calif.	5
4.	Department of Mechanical Engineering Naval Postgraduate School Monterey, Calif.	2
5.	LT Kenneth W. Loveland 75 Seaview Ave., New Rochelle, New York 10801	2
6.	LT S. Phasook Code 34 Naval Postgraduate School Monterey, Calif.	1
7.	RADM Kenneth Loveland, USN (Ret.) 21 Carrol Ave., Vallejo, California	1

DOCUMENT CONTROL DATA - R&D

(Security classification of title, body of abstract and indexing annotation must be entered when the overall report is classified)

1. ORIGINATING ACTIVITY *(Corporate author)*
Naval Postgraduate School, Monterey, California

2a. REPORT SECURITY CLASSIFICATION
Unclassified

2b. GROUP

3. REPORT TITLE
Virtual Mass in Stratified Fluids

4. DESCRIPTIVE NOTES *(Type of report and inclusive dates)*
Thesis

5. AUTHOR(S) *(Last name, first name, initial)*
Loveland, Kenneth W., LT, USN

6. REPORT DATE	7a. TOTAL NO. OF PAGES	7b. NO. OF REFS
June 1968	52	14

8a. CONTRACT OR GRANT NO.	9a. ORIGINATOR'S REPORT NUMBER(S)
N.A.	N.A.
b. PROJECT NO.	
c.	9b. OTHER REPORT NO(S) *(Any other numbers that may be assigned this report)*
d. N.A.	N.A.

10. AVAILABILITY/LIMITATION NOTICES
[redacted]

11. SUPPLEMENTARY NOTES	12. SPONSORING MILITARY ACTIVITY
N.A.	U. S. Navy

13. ABSTRACT

The virtual mass of circular cylinders immersed in a uniformly stratifed nonhomogeneous fluid medium has been investigated both theoretically and experimentally. The experimental equipment consisted of a reservoir filled with one inch thick layers of salt water solution. The density uniformly decreased with elevation (stable stratification). The fluid motion about the cylinder was provided by the standing waves created with a plunger. The resulting velocities and accelerations about the cylinder were harmonic. The theoretical analysis consisted of the calculation of the inertia coefficient through the evaluation of the total kinetic energy of the fluid medium. Use was made of the psuedo-potential flow solution for the stratified flow about a circular cylinder. The results have shown that the inertia coefficient for circular cylinders immersed in a uniformly stratified media is about 25% larger than that for a cylinder immersed in an homogeneous medium.

DD FORM 1 JAN 64 1473

14 KEY WORDS	LINK A		LINK B		LINK C	
	ROLE	WT	ROLE	WT	ROLE	WT
Virtual mass						
Apparent mass						
Inertia coefficient						
Stratified fluids						

thesL834
DUDLEY KNOX LIBRARY
3 2768 00416506 8
DUDLEY KNOX LIBRARY